ACTA IMEKO
ISSN: 2221-870X
September 2023, Volume 12, Number 3, 1 - 9

Characterization, traceability, and uncertainty estimation of reference solar panel module measurements using pulsed solar simulators and reference solar cells

Abdallah M. Karmalawi[1]

[1] *Division of Photometry and Radiometry, National Institute of Standards (NIS), President Sadat St., Al-Haram, Giza, 136, Egypt*

ABSTRACT
This paper presents the design, characterization, and traceability of reference solar panel modules for determining the performance of photovoltaic (PV) modules at standard test conditions (STC). The research introduces an advanced experimental system based on a class AAA pulsed solar simulator to measure the radiometric, electrical performances, and efficiency of PV modules. I-V/P characteristics of three PV modules at different STCs and the associated uncertainty budget of the system were estimated. I-V characteristic and associated parameters including I_{sc}, V_{oc}, P_{max}, *FF*, and efficiency were measured. The radiometric and electrical traceability were discussed, and the relative expanded combined uncertainties were concluded to be 1.62 % (I_{sc}), 0.42 % (V_{oc}), 2.05 % (P_{max}), and 2.5% (η), with a coverage factor k = 2. Reference solar panel modules were also used on-site to test the performance of large PV panels, and the results are reported.

Section: RESEARCH PAPER

Keywords: Solar cells; photovoltaic; solar panels; I-V characteristics; spectral responsivity

Citation: Abdallah Karmalawi, Characterization, traceability, and uncertainty estimation of reference solar panel module measurements using pulsed solar simulators and reference solar cells, Acta IMEKO, vol. 12, no. 3, article 53, September 2023, identifier: IMEKO-ACTA-12 (2023)-03-53

Section Editor: Francesco Lamonaca, University of Calabria, Italy

Received March 24, 2023; **In final form** November 7, 2023; **Published** September 2023

Corresponding author: Abdallah. M. Karmalawi, e-mail: farmalawi_nis@hotmail.com

1. INTRODUCTION

1.1. Introduction to Photovoltaic Panels

Reliance on solar energy as an energy source is the ideal solution as it is harmless to the environment. The average measured amount of solar irradiance that reaches the earth from the sun after passing through the atmosphere on a bright day at sea level is estimated at 1000 W/m^2. Therefore if our rooftops are supplied with solar panels, they can get energy sufficient for daily life requirements, in keeping with the Renewables 2018 Global Status Report. Solar photovoltaic (PV) accounted for 55 % of the new renewable energy setting up in 2017, with a complete global capacity of 402 GW, surpassing fossil fuels as well as nuclear power [1]–[4].

Solar panels themselves do not produce greenhouse gas emissions during their operation, unlike fossil fuel-based energy generation. They contribute significantly to reducing carbon emissions and mitigating climate change. However, it is worth mentioning that the manufacturing process of solar panels does have some environmental impacts, such as the energy and resource requirements for production and the management of waste materials [5]-[7].

To characterize the photovoltaic (PV) modules, sunlight or solar simulators are mainly applied. Furthermore, the international standard IEC 61836 and 60891 explains the standard test conditions (STC) under which the calibration must be accomplished at irradiance intensity of 1000 W/m^2, AM 1.5G solar reference spectrum, and device temperature of 25 °C [8]-[10]. According to the STC, the solar cells or solar panels can be measured/tested either indoor or outdoor sits; however, the solar simulator has some disadvantages over natural sunlight, for example, the cost, the light source used may be required a high power to run, in addition to the ozone gas may be produced by the lamp and spectrum mismatching. In contrast, the advantage of the outdoor solar experiment is that the operation in the real conditions of a solar installation and direct sunlight can avoid the spectral mismatch problem. But since the natural sunlight varies from time to time and maybe not be available every day, most laboratories and manufacturers use an indoor method using solar simulators [11], [12].

The proper management and regulation of the current source within the range of zero current points (V_{oc}) and the short circuit point (I_{sc}) is essential for accurately measuring the *I-V* curve of a photovoltaic (PV) solar cell. Various techniques have been proposed to achieve this management, including the utilization of variable resistors, capacitive loads, electronic loads, bipolar power amplifiers, and four-quadrant power supplies. These techniques enable effective detection and control of the current source, ensuring precise characterization of the *I-V* curve.

From the calibration of solar modules' *I-V* characteristic parameters traceable to SI units [9], the *I-V* characteristic is a crucial link in the entire traceability chain of the solar cells industry. To date, no one in the world has recorded the entire chain of traceability for photovoltaic industries. PTB and KRISS [13]-[16] concentrate on primary reference solar cell calibration, while NIST focuses on functional measurements and other properties studies for solar cells and modules. We will present a measurement method for solar cells' *I-V* characteristic calibration based on the traceable chain at standard test conditions as well as at different test conditions at 1000 W/m², 800 W/m², and 200 W/m² [4].

1.2. Maximizing Solar Potential in Aswan: Aswan Solar Park

According to the Global Solar Atlas data, Egypt is one of the promising countries in the world that have great resources for PV power as clean energy (see Figure 1).

Egypt has taken an early series of steps to minimize its dependency on the barrel of oil and achieve a balance between development and climate change, where Egypt targets 37 % of clean energy by 2035. One of these steps is establishing a large solar park. In Egypt the largest solar park in Africa, Benban solar park located near Aswan, southern Egypt (see Figure 2). Benban solar park was built on an area of 40 km² as can see in Figure 2.

Aswan Solar Park is a large-scale solar power plant located in Aswan, Egypt. It is considered one of the largest solar parks in the world, with a total capacity of 1.8 GW. In terms of global solar radiation, Aswan is located in a region with high solar irradiance, which makes it an ideal location for solar power generation.

When comparing Aswan's global solar radiation to other locations, it is essential to consider factors such as latitude, altitude, and climate. According to data from the World Radiation Data Centre (WRDC), Aswan has an average annual global solar radiation of around 2,300 kW h/m², which is relatively high compared to other locations worldwide. For instance, the average annual global solar radiation in Germany is around 1,100 kW h/m², while in the United States, it ranges from 1,300 kW h/m² in the Northeast to 2,800 kW h/m² in the Southwest in Figure 3, comparison of photovoltaic potential power between in Germany and Egypt [18].

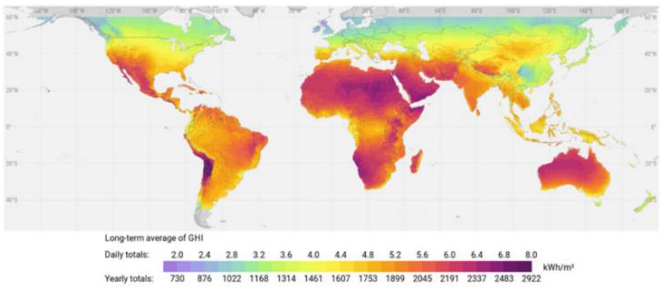

Figure 1. Global Horizontal Irradiation (GHI): Long-term yearly average of daily and yearly totals [17].

However, Aswan's global solar radiation is still lower than some of the world's sunniest locations, such as the Sahara Desert in Algeria and the Atacama Desert in Chile. These areas receive annual solar irradiance of around 2,800 kW h/m² - 3,000 kW h/m².

In terms of evaluating the performance of Aswan Solar Park, several factors need to be considered, including the efficiency of the solar panels, the capacity factor, and the levelized cost of energy (LCOE). The efficiency of the solar panels used in Aswan Solar Park is typically between 15 % - 20 %, which is considered reasonable for large-scale solar power plants [19].

The capacity factor of Aswan Solar Park varies depending on the time of the year and weather conditions. During the summer months, when solar irradiance is high, the capacity factor can be as high as 35 % - 40 %, while during the winter months, it can drop to around 20 % - 25 %.

The levelized cost of energy (LCOE) of Aswan Solar Park is relatively low, estimated at around 3 to 4 US cents per kW h. This is due to the favourable conditions for solar power generation in the region, which allows for higher energy output and lower operational costs.

Overall, Aswan Solar Park benefits from high solar irradiance levels, which contribute to high energy output and low LCOE. However, to fully evaluate its performance, other factors such as efficiency, capacity factor, and operating costs should also be considered.

1.3. Research Goals

The primary objective of measuring and computing solar radiation is to ascertain the amount of electrical energy that can be produced within a specified period. Therefore, in this study, we aim to demonstrate how the models of solar radiation and its components enable us to comprehend and evaluate the efficiency of solar power facilities.

Figure 2. Google map of Banban solar park in Aswan, Egypt.

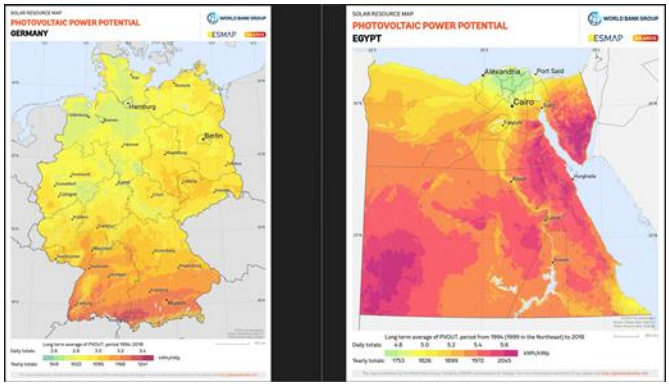

Figure 3. Photovoltaic power potential between Germany and Egypt [18].

In this paper; a pulsed xenon solar simulator is used as an irradiation source to measure the *I-V* curve of reference solar panels; the efficiency and some related parameters of the P.V. panels (which depend mainly on solar insolation or irradiance (G), cell temperature (T_c), series resistance (R_s), and shunt resistance (R_{sh}) were measured and calculated as (I_{sc}), (V_{oc}) and (P_{max}). The maximum power (P_{max}) derived from the PV cell, or its full operating power depends on the load resistance (R). Additionally, the traceability of the calibration of the reference solar cells has been discussed, and the uncertainty budget of *I-V* measurements is estimated and evaluated in detail.

Regarding the research goal, our primary objective is to assess the characterization, traceability, and uncertainty estimation of reference solar panel module measurements. By conducting this evaluation, we aim to enhance the understanding and reliability of these measurements, ultimately contributing to the accuracy and consistency of solar energy assessments.

Many efforts have been made by many researchers and practitioners in the field of solar cells regarding the measurement and testing of solar panels, but the traceability of these measurements and how it is trusted and reliable have some leakage. In this paper, we're showing comprehensive results that can be useful for those who are interested in solar panel measurements, and at the same time, they are having lacked in the metrology background of a photovoltaic system. In this research, we present in detail the performance of the pulsed solar simulator, the *I-V* characteristic of solar panels and its correlated uncertainty estimation, and the uncertainty budget of solar panel measurements.

In this paper we measured and characterised reference solar panel modules that are used as a standard for measuring the performance of other solar panel modules. They are calibrated to known values of key parameters such as current, voltage, and power output, and are used as a benchmark for comparison with other modules. By using reference modules, the performance of different modules can be compared in a standardized and objective manner, regardless of their make or model. This allows for accurate and reliable evaluation of the performance of different solar panel modules, which is important for the development and improvement of solar energy technology.

2. I.V CHARACTERIZATION SYSTEM OF REFERENCE PHOTOVOLTAIC MODULE

Solar simulators are tested and graded as part of the indoor testing phase using industry criteria [8]. The spatial uniformity, temporal stability, and spectral irradiance distribution of the solar simulator were used to classify it [10]. The solar simulator's efficiency is determined by three factors. According to ASTM E927-5, it can be classified as class A, B, or C, with spectral mismatch, irradiance uniformity, and stability being the three groups [20], [21].

The spectral mismatch is the ability and how the solar simulator spectrum is matching with natural sunlight. Irradiance uniformity dives into the uniformity and homogeneity of the solar simulator over the photovoltaic module's illuminated area, depending on the application used. The third class is the stability of the solar simulator, and it is the temporal stability of the emitted irradiance over a specific time.

The system consists of three central units, as shown in Figure 4. The first unit is responsible for the electrical performance measurement of the photovoltaic module and irradiance measurement, the second unit is pulsed flash sun

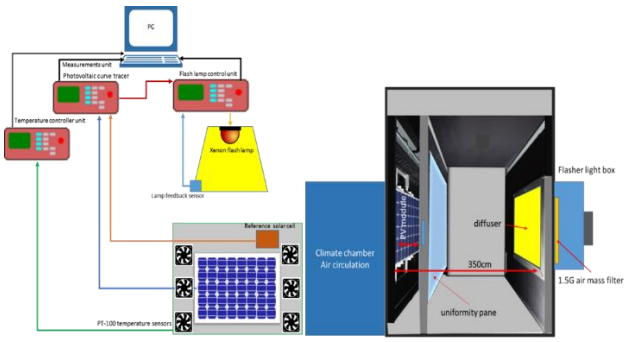

Figure 4. The schematic layout of the I-V characteristic measurement setup for solar panel modules over a pulsed solar simulator.

simulator control, and the third part is the unit that controls temperature, air circulation control, and temperature measurement.

A xenon flash lamp is located outside the black enclosure of the pulsed solar simulator. The pulsed flash lamp is operated by a load capacitor discharge with a pulse duration of about 37 milliseconds; this simulator, as shown in Figure 5, has a pulse duration of about 37 milliseconds and can cover solar panel modules measuring 2.1 m by 1.6 m. The pulsed flash source has features that extend its measurement capabilities; for example, the spectral irradiance can be adjusted by changing the stored capacitive charge.

During the pulsed flash length, a high-speed data acquisition device collects the signal output from the solar panel module. This data acquisition arrangement delivers a pulsed trigger signal that can synchronize all attached external equipment and simultaneously start the measurement of I-V curve, irradiance levels, and temperature. This flash light box including the xenon lamp was connected with irradiance monitor feedback, this feedback signal control and adjust the irradiance levels according to user requirements.

3. PULSED SOLAR SIMULATOR PERFORMANCE

The pulsed solar simulator is demand rather than the continuing sources; the pulsed solar simulator was designed to prevent heat build-up in the solar panels generated by the lamp. According to the International Electrotechnical Commission (IEC) Standard 60904-9 [22], any photovoltaic solar simulator's overall performance as well as characterization outputs are

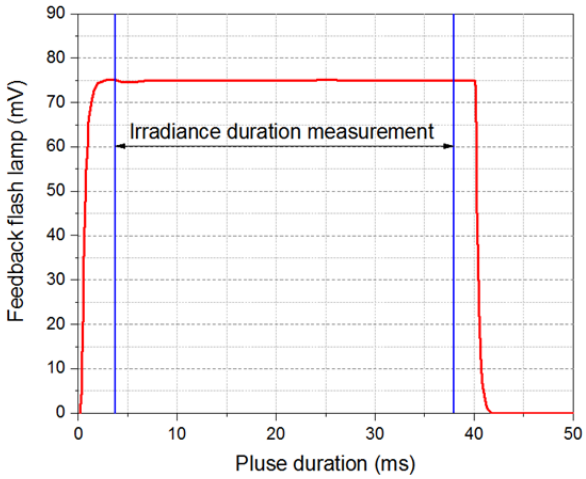

Figure 5. Feedback of pulsed solar simulator duration.

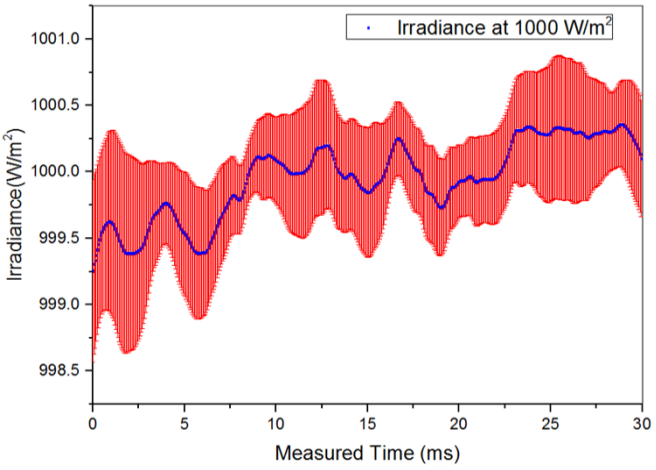

Figure 6. Irradiance detection stability throughout a single pulse detected via a solar cell based on a single air mass AM1.5G (Red error bar indicates the irradiance's standard deviation).

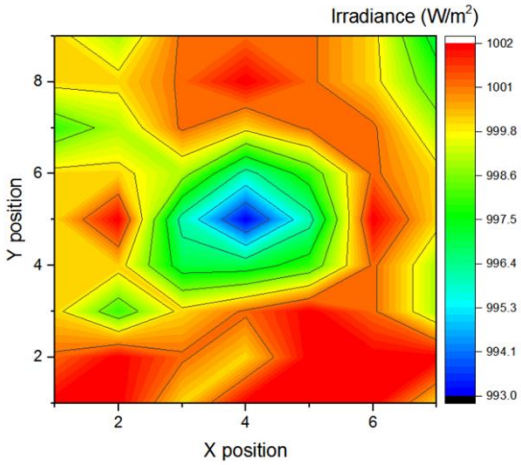

Figure 7. Spatial consistency of the pulsed solar simulator was detected with a calibrated reference solar cell at 63 points at altered grid sites inside the test plane of the PV modules.

estimated depending on three categories: temporal stability, spatial uniformity, and spectral distribution. Furthermore, the pulsed solar simulator's temporal stability or irradiance stability refers to irradiance (W/m²) adjustments at some point in the pulse duration. Results of pulse-to-pulse stability are correspondingly detected, as illustrated in Figure 4. In addition, Figure 6 displays the irradiance stability of 1000 W/m² for the flashlight duration of 30ms, the standard irradiance deviation during this pulse duration is about 0.059 % (temporal flash stability < ±0.5 % (class A+, according to IEC 60904-9 Ed.2)).

The spatial uniformity of the pulsed solar simulator, as found in Figure 7, was measured preform consecutive experiments using a reference solar cell to detect the total irradiance at 63 points at dissimilar grid positions inside the test plane of the PV modules. The spatial uniformity measured for the central 210 cm by 140 cm test plane gave a non-uniformity of 0.90 %, which indicates that the pulsed solar simulator was classified as an "A" class (Non-uniformity < ±1 % (class A+, IEC 60904-9 Ed.2).

The spectral mismatch of the pulsed solar simulator spectrum from the standard spectrum AM1.5G combined with the difference between the reference cell's spectral response and that of the device under test (DUT) was calculated based on equation (1) and corrected accordingly. For the spectral mismatch correction, the spectral distribution of the pulsed solar simulator is measured with a spectroradiometer. The spectral response of the reference solar cells and DUT is measured with a double monochromator device.

Due to the spectral response of the reference solar cell varies from the test cell or module, the mismatch factor was calculated from:

$$M = \frac{\int E(\lambda)\cdot S_t(\lambda)\,\mathrm{d}\lambda \int E_o(\lambda)\cdot S_r(\lambda)\,\mathrm{d}\lambda}{\int E_o(\lambda)\cdot S_t(\lambda)\,\mathrm{d}\lambda \int E(\lambda)\cdot S_r(\lambda)\,\mathrm{d}\lambda}, \quad (1)$$

where $S_r(\lambda)$ is the reference device spectral responsivity, $S_t(\lambda)$ the test device spectral responsivity, $E_o(\lambda)$ is the global AM1.5 reference spectral distribution, and $E(\lambda)$ is the solar simulator spectral distribution.

In addition, Table 1 reports the deviation of the spectral match of our solar simulator from the ideal Spectral match defined by IEC 60904-9 and JIS C 8904-9.

As shown in Figure 8, the spectral mismatch of the solar is measured and calculated according to the equation above. The relative spectral match deviation was found to be about 8.5 % to -5.36 % with an average of about 0.3 %, depending on the spectral wavelength according to IEC 60904-9, the

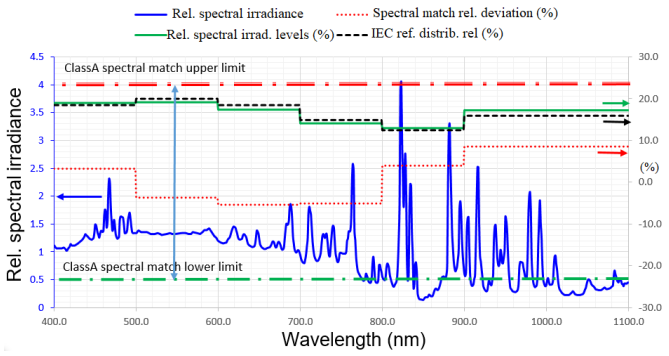

Figure 8. The spectral variation of solar simulators (cetisPV-XF2) (relative Spectral match deviation from JIS/IEC irradiance distribution in %).

Table 1. Performance validation of cetisPV-XF2 pulsed solar simulator (relative Spectral match deviation from JIS/IEC irradiance distribution in %).

Wavelength/nm	Measured relative irradiance distribution (%)	JIS/IEC ref. distribution rel. (%)	Difference (measured irradiance - IEC)	Spectral match rel. deviation (%)	IEC grade (Class)
400-499	19.00	18.4	0.60	3.27	A
500-599	19.17	19.9	-0.73	-3.65	A
600-699	17.41	18.4	-0.99	-5.36	A
700-799	14.15	14.9	-0.75	-5.06	A
800-899	13.00	12.5	0.50	4.01	A
900-1100	17.26	15.9	1.36	8.58	A

characterization of solar simulators has a spectral variation within ± 25 % as compared to the standard AM1.5 spectrum is classified as class A simulator.

The short-circuit current measurements of such solar panel can be corrected using the following equation based on the short circuit of the reference solar cell ($I_{SC\ REF}$) in addition to the spectral response mismatch (M):

$$I_{SC} = \frac{I_{SC\ REF}}{M+1}. \quad (2)$$

The measurement of the traceability of the spectral distribution is achieved using a standard lamp for the calibration of the spectroradiometer. The pulsed solar simulator's spectral distribution was measured using a CCD spectroradiometer over the spectral range of 300 nm – 1100 nm (with a relative uncertainty of about 3 %); in turn, it was calibrated against the FEL standard light lamp and mercury/xenon spectrum light sources. According to IECO60904-9 ed.2, the results of the spectral irradiance and spectral match for each wavelength region, the solar simulator rated as class A++ under standard test conditions STC.

4. TRACEABILITY OF THE REFERENCE SOLAR CELL AND SOLAR IRRADIANCE MEASUREMENT

Previous studies have recorded the measurement traceability of solar cells to the International System of Units (SI) [16], [23]. The electrical replacement radiometer (Cryogenic Radiometer) is used at the very top of the traceability chain to calibrate Si-trap detectors, which are then used to calibrate other detector radiometers for the realizations of the spectral irradiance scale and the detector's responsivities [24]–[27].

The spectral responsivities of the reference solar cells, SR (λ), are applied to measure the spectral irradiances of the solar simulator at an air mass of 1.5 G; and these reference solar cells have calibrated against the Si-tap detector over NIS's spectral responsivity facilities, as demonstrated in Figure S1, in the supporting information (SI) as mentioned in our previous study [27].

Solar cell and photovoltaic module calibration involve determining the short-circuit current of the device produced by a reference solar radiation with 1 kW m^{-2} total irradiance and a reference solar spectral irradiance distribution. However, the calibration value may be affected by double spectral mismatch between the test and standard device, as well as between the test and reference solar spectrum, and by non-linearity effects when transferring the calibration from low to high irradiance levels.

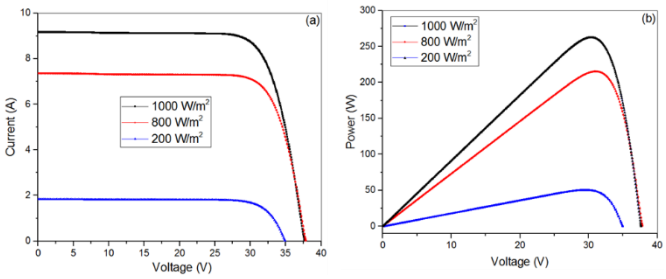

Figure 9. (a) *I-V* curve and (b) Output Power from the PV Module "A" with different irradiance levels.

5. VALIDATION OF SOLAR RADIATION MODEL

Numerous attempts have been made to assess solar radiation, and one of the valuable models for estimating clear sky solar irradiance in DHI, DNI, and GHI irradiance modes is CLIRAD-SW. This model was created by NASA [28]-[30].

The validation of the solar radiation model was developed and operated by the Solargis model [31]. Validation of the irradiance model has been performed using data from professional public networks of ground measurement stations, and also solar measurements acquired within the measurement.

Solargis model data has been utilized to measure and validate various irradiance modes. However, the accuracy of these measurements may be impacted by several limiting factors such as the geographical location, local climate, and geographic features. Solargis provides a range of solar radiation parameters, including Global Horizontal (GHI), Direct Normal (DNI), Diffuse Horizontal (DIF), and Global Tilted Irradiance (GTI).

6. RESULTS & DISCUSSIONS

Figure 9 and Table 2 show the I-V and P-V characteristics of the Polycrystalline solar panel module, the measurements were carried out at different irradiance levels 1000 W/m² (STC test at 25 °C), 800 W/m² (NMOT test at 20 °C), and 200 W/m² (Low irradiance test at 25 °C).

The correction for current and voltage, according to STC, are given in the following equations:

$$T_{STC} = I_m + \left[\frac{1000\ \mathrm{W/m^2}}{E_m} - 1\right] I_{SC,m} + \alpha \cdot (T - 25\ °C) \quad (3)$$

$$V_{STC} = V_m - R_S\,(I_{STC} - I_m) - K\,I_{STC}\,(T - 25\ °C) + \beta\,(T - 25\ °C)\,, \quad (4)$$

Table 2. *I-V* characterization parameters for three solar panels module at different test conditions.

Module	Irradiance W/m²	I_{SC}(A)	V_{OC}(V)	P_{mpp}(W)	I_{mpp}(A)	V_{mpp}(V)	F.F.	η %
A	1000	9.17	37.65	262.75	8.64	30.40	76.11	15.46
	800	7.36	37.84	215.46	6.95	31.01	77.34	15.83
	200	1.84	34.94	50.80	1.72	29.52	79.07	14.89
B	1000	9.01	38.17	266.86	8.51	31.35	77.61	15.70
	800	7.24	38.35	218.00	6.83	31.86	78.55	16.03
	200	1.81	35.39	50.83	1.69	30.02	79.30	14.90
C	1000	9.08	38.19	268.59	8.56	31.37	77.50	15.80
	800	7.28	38.39	219.60	6.87	31.95	78.53	16.15
	200	1.83	35.45	51.26	1.71	30.02	79.16	15.08

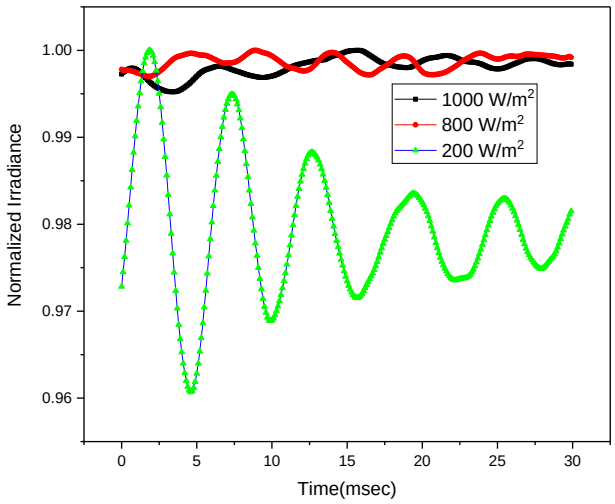

Figure 10. Stability of the pulsed solar simulator during measurement time at different irradiance levels.

where, I_m and V_m are the measured current and voltage respectively, α is the temperature coefficient for ISC, β is the temperature coefficient for V_{OC}, R_S is the series resistance, and K is the curve correction factor.

In this section, we explain the uncertainty sources related to the PV module; the uncertainty estimation was performed according to the "Guide to the expression of uncertainty in measurement" [32].

The uncertainty sources of photovoltaic modules' performance arise from many parameters; parameters are ceased by the pulsed solar simulator, reference solar cells, electrical sources, and environmental factors. The uncertainty associated with the solar simulator's performance can be summarized in a few factors, uncertainty factors caused by irradiance instability of flash lamp, spectrum mismatch, non-uniformity of the solar simulator, etc.

To estimate the uncertainty due to spectrum mismatch, the uncertainties of the reference solar cell, PV module spectral responsivity, and the relative spectral distribution of the pulsed solar simulator have to determine. The spectral mismatch of the system is calculated to be 0.999, with an uncertainty of about 0.3 %.

The pulsed solar simulator's spatial no uniformity was recorded at about 0.90 %, with an associated uncertainty of 0.19 %. The uncertainty due to Irradiance temporal stability (for 35 s) at irradiance level around 1000 W/m² was about 0.059 %.

The dominant error sources of the IV characteristics of such solar panels come from pulsed flashlight spectral mismatch, lamp source fluctuations, reference solar cell calibration uncertainty, spatial uniformity of the beam light, and temperature variation. The solar simulator error's spatial uniformity significantly impacts the reference solar cell, and the solar panel module under test is not the same size. It is not in the same position where the irradiance value changed from point to point.

The stability of the pulsed solar simulator has some variation. The division from the nominal value has been observed mainly for low irradiance value as shown in Figure 10; according to these divisions in the irradiance, the non-uniformity accordingly became more noticeable. This, in turn, increases the uncertainty values; for example, the uncertainty related to the I_{sc} can vary from 1.6 % up to 3 % depending on the irradiated area uniformity.

The selection criteria of the tested modules have to meet the following formula [33]:

$$Par_{\max}(Lab)\cdot\left[1+\frac{|m_1|(\%)}{100}\right]\geq Par_{\max}(NP)\cdot\left[1-\frac{|t_1|(\%)}{100}\right] \quad (5)$$

where, $Par_{\max}(Lab)$ could be the maximum I_{sc}, V_{oc}, or $P_{\max}$ of each module in the stabilized state; $Par_{\max}(NP)$ could be the maximum rated nameplate I_{sc}, V_{oc}, or $P_{\max}$ of each module without tolerances; m_1 is the measurement uncertainty of laboratory; t_1 is the manufacturer's rated lower production tolerance.

Table 3 shows the uncertainty budget for a polycrystalline solar module; the table was divided into five main parameters, reference cell (Fraunhofer ISE reference cell), pulsed solar simulator, DC voltage, current measurements, and uncertainty of temperature measurements.

The short-current value I_{sc} is measured by measuring the voltage drop across a series of shunt resistors with a digital precision measuring system with an uncertainty value of 4.5×10^{-6} to 7.5×10^{-5}. For DC voltage measurements, the data acquisition has seven ranges covering from isolator to ± 200 V with average uncertainty of 3.7×10^{-5}, and the uncertainty due to the scale range of ± 0.0014 %.

The relative expanded uncertainty was calculated and the uncertainty was founded due to an error caused by irradiance levels for V_{OC} can be neglected. Thus, the factors that impact the open-circuit voltage are mainly the voltage reading device for a specific range and its correlated temperature correction.

The Performance Ratio can be calculated as the ratio between the actual delivered outputs and the targeted energy that would have been generated.

$$PR_{\text{meas}}=\frac{\sum_j ADO_j}{\sum_j E_{\text{module}_j}}\cdot 100\,, \quad (6)$$

where the target output energy can be expressed as,

$$E_{\text{module}_j}=PA\left\{\frac{G_j}{1000}\cdot\frac{MI}{60}\cdot\frac{\eta_{\text{STC}}}{100}\left[1-\frac{\beta}{100}\left(T_{\text{mod}_n}-T_{\text{Meas}_j}\right)\right]\right\}. \quad (7)$$

Here, MI is the irradiance GHI (W h/m²), η_{STC} is the PV module efficiency, β is the temperature coefficient, and PA is the total PV area.

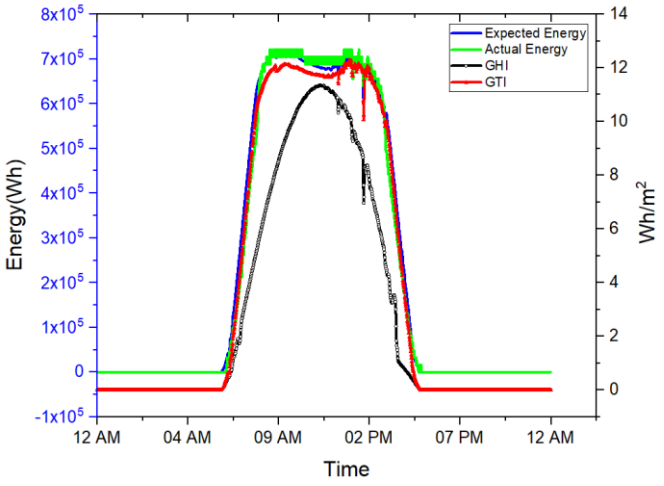

Figure 11. Relation between expected and actual output energy and the irradiance modes.

Table 3. The uncertainty parameters for a polycrystalline solar module.

Uncertainty Component	Distribution type	Relative standard uncertainty in %
1. Reference cell (Fraunhofer ISE reference cell)		**1.06**
Spectral Responsivity(certificate)	Normal (*k*=1)	0.50
Reference cell signal(repeatability)	Normal	0.0010
Non-linearity of the reference cell	Rectangular	0.00001
Reference cell multimeter	Rectangular	0.015
Measured *Isc* of the reference cell	Rectangular	0.94
Reference cell drift	Rectangular	0.0020
2. Pulsed solar simulator		**0.36**
Spatial non-uniformity	Rectangular	0.18655
Spectral Mismatch (includes the uncertainties of the reference cell, SR of the module, and relative spectral distribution of the pulsed solar simulator) STC	Normal	0.30
Monitor cell amp(certificate)	Normal (*k*=2)	0.00038
Dark background (for 10 s)	Normal	0.03132
Irradiance Temporal stability (for 35 s)	Normal	0.05924
Area measurements	Normal	0.50
3. Uncertainty of DC voltage measurement		**0.0019**
DC voltage Signal repeatability	Normal	0.00190
Voltage DAQ (certificate)	Normal (*k*=2)	0.00002
4. Uncertainty of DC current measurement		**0.0008**
Ohmic resistance calibration (certificate)	Normal (*k*=2)	0.6 (μΩ/Ω)
Resistor 1-year stability	Rectangular	
DC Signal (DAQ) calibration (certificate)	Normal (*k*=2)	0.00077
5. Uncertainty of temperature measurement		**0.36**
Pt100 calibration	Normal (*k*=2)	0.00015
The signal from (DAQ)	Normal	0.30
Temperature non-uniformity	Rectangular	0.20

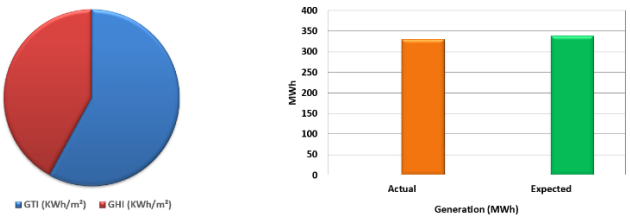

Figure 12. (a) Average irradiation of GTI and GHI for one day, (b) Exported energy of actual and expected output.

Figure 11 provides a comprehensive representation of the relationship between various variables: expected output electricity, actual output electricity, GHI (Global Horizontal Irradiance), and GTI (Global Tilted Irradiance) irradiance modes. The figure visually demonstrates how these factors interrelate.

By examining Figure 11 and Figure 12, we can observe the following insights: The expected output electricity is compared to the actual output electricity, allowing for an assessment of their relative performance. Additionally, the irradiance modes, specifically GHI and GTI, play a crucial role in influencing the electricity output. The figure enables a clear understanding of how these irradiance modes impact the electricity generation process.

Recently, we have constructed several facilities to provide traceability for solar cell and pyranometer calibration, as reported in the research paper [23], [34]-[36].

7. CONCLUSIONS

This research is considered a guide for those working on testing and measuring large solar panels; in this paper, each contribution to the total measurement uncertainty was investigated individually to obtain a complete description of the resulting uncertainty of the solar panel system. We are focusing on the radiometric performance of the solar simulators as the stability, calculating the spectral mismatch and non-uniformity. Furthermore, the indoor pulsed solar simulator and the measurement devices were described. Besides, the *I-V* characteristic of P.V. modules at different standard test conditions have been measured and the associated uncertainty budget of the system has been evaluated.

The *I-V* characteristic and associated parameters as I_{sc}, V_{oc}, P_{max}, F.F., and efficiency of solar panel modules were measured at STC, i.e., spectral irradiance AM 1.5 G, 1000 W/m² irradiance, and device temperature of 25 °C. Additionally, a comparative consumed combined uncertainty U_{rel} of 1.62 %, (I_{sc}), 0.42 % (V_{oc}), 2.05 % (P_{max}) and efficiency η of 2.5 % was concluded, with a coverage factor $k = 2$.

REFERENCES

[1] International Energy Agency, Solar Energy Mapping the road ahead, 2019. Online [Accessed 14 September 2023] https://www.iea.org/reports/solar-energy-mapping-the-road-ahead

[2] V. Petrova-Koch, R. Hezel, A. Goetzberger, High-efficient low-cost photovoltaics, Springer Berlin, Heidelberg, (2009),ISBN 978-3-540-79359-5.
DOI: 10.1007/978-3-540-79359-5

[3] Ren21, A. Zervos, C. Lins, Renewables 2017 global status report. Online [Accessed 14 September 2023] https://www.ren21.net/wp-content/uploads/2019/05/GSR2017_Full-Report_English.pdf
[4] K. Terashima, H. Sato, T. Ikaga, Development of an environmentally friendly PV/T solar panel, Sol. Energy 199, (2020), 510–520. DOI: 10.1016/j.solener.2020.02.051
[5] M. Vácha, J. Kodymová, V. Lapčík, Life-cycle assessment of a photovoltaic panel: Assessment of energy intensity of production and environmental impacts, IOP Conf. Ser. Mater. Sci. Eng. 1209, (2021), 012027. DOI 10.1088/1757-899X/1209/1/012027
[6] A. Jäger-Waldau, I. Kougias, N. Taylor, C. Thiel, How photovoltaics can contribute to GHG emission reductions of 55% in the EU by 2030, Renew. Sustain. Energy Rev. 126, (2020) 109836. DOI: 10.1016/j.rser.2020.109836
[7] V. Masson, M. Bonhomme, J. L. Salagnac, X. Briottet, A. Lemonsu, Solar panels reduce both global warming and urban heat island, Front. Environ. Sci. 2, (2014). 1–10. DOI: 10.3389/fenvs.2014.00014
[8] IEC, IEC TS 61836:2016 Solar Photovoltaic Energy Systems - Terms and Symbols. Online [Accessed 14 September 2023] https://webstore.iec.ch/publication/28612
[9] J. Lopez-Garcia, D. Pavanello, T. Sample, Analysis of temperature coefficients of bifacial crystalline silicon pv modules, IEEE Journal of Photovoltaics, 8 (2018), pp. 960-968. DOI: 10.1109/jphotov.2018.2834625
[10] IEC, IEC 60891:2021 Photovoltaic devices - Procedures for temperature and irradiance corrections to measured I-V characteristics. Online [Accessed 14 September 2023] https://webstore.iec.ch/publication/61766
[11] D. M. Atia, H. T. El-Madany, A. Eliwa, A. Samir, M. Zahran, K. El-Metwally, A. Mahgoub, Spectral irradiance estimation of light emitting diode solar simulator based on genetic algorithm, Research Journal of Applied Sciences, Engineering and Technology 15 (2018), pp. 227–235. DOI: 10.19026/rjaset.15.5862
[12] A. Gallo, A. Marzo, E. Fuentealba, E. Alonso, High flux solar simulators for concentrated solar thermal research: A review, Renewable and Sustainable Energy Reviews 77 (2017), pp. 1385–1402. DOI: 10.1016/j.rser.2017.01.056
[13] Seung Kyu Ahn, Se Jin Ahn, Jae Ho Yun, Dong-Hoon Lee, Stefan Winter, Sanekazu Igari, KyungHoon Yoon, Establishment of a primary reference solar cell calibration technique in Korea: methods, results and comparison with WPVS qualified laboratories, Metrologia 51 (2014), pp. 139–147. DOI: 10.1088/0026-1394/51/3/139
[14] Petri Kärhä, Hans Baumgartner, Janne Askola, Kasperi Kylmänen, Benjamin Oksanen, Kinza Maham, Vo Huynh, Erkki Ikonen, Measurement setup for differential spectral responsivity of solar cells, Optical Review 27 (2020), pp. 195–204. DOI: 10.1007/s10043-020-00584-x
[15] S. Winter, T. Fey, I. Kröger, D. Friedrich, K. Ladner, B. Ortel, S. Pendsa, D. Schlüssel, Design and realization of a next generation high accuracy primary calibration facility for solar cells at PTB, XX IMEKO World Congress, Busan, Republic of Korea, 9-12 September 2012. Online [Accessed 5 May 2023] https://www.imeko.org/index.php/proceedings/3188-design-and-realization-of-a-next-generation-high-accuracy-primary-calibration-facility-for-solar-cells-at-ptb
[16] S. Winter, T. Fey, I. Kröger, D. Friedrich, K. Ladner, B. Ortel, S. Pendsa, F. Witt, Design realization and uncertainty analysis of a laser-based primary calibration facility for solar cells at PTB, Measurement, Volume 51, (2014), 457-463. DOI: 10.1016/j.measurement.2013.12.001
[17] IEA-PVPS T1-37:2020, Snapshot of Global PV Markets, 2020. Online [Accessed 14September 2023] https://iea-pvps.org/snapshot-reports/snapshot-2020/
[18] Solargis. Online [Accessed 5 May 2023] https://solargis.com/maps
[19] A. S. A. Mohamed, Hussein M. Maghrabie, Techno-economic feasibility analysis of Benban solar Park, Alexandria Engineering Journal, vol. 61, issue 12, (2022), pp. 12593-12607. DOI: 10.1016/j.aej.2022.06.034
[20] ASTM E927-05, Dec 31, 2010, Standard Specification for Solar Simulation for Terrestrial Photovoltaic Testing. Online [Accessed 14 September 2023] https://www.astm.org/e0927-05.html
[21] A. Georgescu, M. A. Gîrţu, V. Ciupină, Spectral calibration of a LED–based solar simulator – a theoretical approach, Journal of optoelectronics and advanced materials, Vol. 15, No. 1-2, January-February 2013, pp. 31–36. Online [Accessed 14 September 2023] https://joam.inoe.ro/articles/spectral-calibration-of-a-ledbased-solar-simulator-a-theoretical-approach/
[22] IEC, IEC 60904-9:2020, Photovoltaic devices - Part 9: Classification of solar simulator characteristics. Online [Accessed 14 September 2023] https://webstore.iec.ch/publication/28973
[23] Esraa M. El-Mahdy; Samira Abd El-Mongy; Abdallah M. Karmalawi. Apparatus for calibration of photovoltaic cells at National Institute of Standards. IEEE Instrumentation & Measurement Magazine (Vol. 25, Issue 3), (2022) 22 - 29. DOI: 10.1109/MIM.2022.9759359
[24] L. Werner, J. Hartmann, Calibration and interpolation of the spectral responsivity of silicon photodiode-based detectors. Sensors Actuators A Phys. 156 (2009), pp. 185–190. DOI: 10.1016/j.sna.2009.05.002
[25] J. Campos, A. Pons, P. Corredera, Spectral responsivity scale in the visible range based on single silicon photodiodes. Metrologia 40 (2003), S181–S184. DOI: 10.1088/0026-1394/40/1/341
[26] Y. S. Yoo, G. J. Kim, S. Park, D.-H. Lee, B.-H. Kim, Spectral responsivity calibration of the reference radiation thermometer at KRISS by using a super-continuum laser-based high-accuracy monochromatic source, Metrologia, 53(6), pp. 1354–1364. DOI: 10.1088/0026-1394/40/1/341
[27] A. M. Karmalawi, A. A. Abdelmageed, Development of a detector-based absolute spectral power responsivity scale in the spectral range of 300–1600 nm. J Mater Sci: Mater Electron 32 (2021), pp. 5215-5221. DOI: 10.1007/s10854-021-05253-6
[28] Chou Ming-Dah, Suarez Max J, A Solar Radiation Parameterization for Atmospheric Studies, NASA/TM-1999-104606, Vol. 15, (1999). Online [Accessed 14 September 2023] https://ntrs.nasa.gov/citations/19990060930
[29] T. A. Tarasova, Boris Fomin, The use of new parameterizations for gaseous absorption in the CLIRAD-SW solar radiation code for models, Journal of Atmospheric and Oceanic Technology 24(6) (2007), pp. 1157- 1162. DOI: 10.1175/JTECH2023.1
[30] H. M. J. Barbosa, T. A. Tarasova, New solar radiation parameterization in CPTEC/COLA GCM, Proc. of 8 ICSHMO, Foz do Iguaçu, Brazil, 24-28 April 2006, INPE, pp. 493-494. Online [Accessed 14 September 2023] http://www.fap.if.usp.br/~hbarbosa/uploads/Site/Publications/8ICSHMO_Henrique_493-494.pdf
[31] T. Cebecauer, M. Suri, Typical Meteorological Year data: SolarGIS approach, International Energy Procedia 69 (2015), pp. 1958 – 1969. DOI: 10.1016/j.egypro.2015.03.195
[32] JCGM 100:2008, Evaluation of measurement data — Guide to the expression of uncertainty in measurement. Online [Accessed 14 September 2023] https://www.bipm.org/documents/20126/2071204/JCGM_100_2008_E.pdf

[33] IEC, IEC 61215-1-1: 2021 Standard, Terrestrial photovoltaic (PV) modules - Design qualification and type approval - Part 1-1: Special requirements for testing of crystalline silicon photovoltaic (PV) modules. Online [Accessed 14 September 2023] https://webstore.iec.ch/publication/61346

[34] A. Karmalawi, Radiometric Traceability for Pyranometer Calibration Based on High Flux LEDs and Reference Detector, Indian Journal of Pure & Applied Physics, Vol. 61, No. 4, (2023), pp. 247-253. DOI: 10.56042/ijpap.v61i4.68963

[35] Abdallah M. Karmalawi, Diaa A. Rayan, Mohamed M. Rashad, Establishment and evaluation of photovoltaic quantum efficiency system at central metallurgical research and development institute, Optik - International Journal for Light and Electron Optics 217 (2020), 164931. DOI: 10.1016/j.ijleo.2020.164931

[36] A. M. Karmalawi, Radiometric Traceability for Pyranometer Calibration Based on High Flux LEDs and Reference Detector, Indian Journal of Pure & Applied Physics (IJPAP) 61.4 (2023), pp. 247-253. DOI: 10.56042/ijpap.v61i4.68963